IEEE Access
Multidisciplinary | Rapid Review | Open Access Journal

Received March 1, 2019, accepted March 18, 2019, date of publication March 26, 2019, date of current version April 12, 2019.

Digital Object Identifier 10.1109/ACCESS.2019.2907569

Model-Matching Fractional-Order Controller Design Using AGTM/AGMP Matching Technique for SISO/MIMO Linear Systems

SURAJ DAMODARAN[1], THAZHE KUNNATH SUNIL KUMAR[1], AND ATTADAPPA PUTHANVEETIL SUDHEER[2]

[1]Department of Electrical Engineering, National Institute of Technology Calicut, Kozhikode 673601, India
[2]Department of Mechanical Engineering, National Institute of Technology Calicut, Kozhikode 673601, India

Corresponding author: Suraj Damodaran (surajdamodaran@gmail.com)

ABSTRACT A new two-stage method is proposed for the model-matching fractional-order (FO) controller (FOC) design for the single-input single-output (SISO) / multiple-input multiple-output (MIMO) linear systems. A streamlined procedure for the selection of reference model M(s), based on a linear quadratic regulator (LQR) with integral action (LQRI) is presented. Since the proposed M(s) is designed using the optimal control theory, the designed output-feedback closed-loop system can be termed as a suboptimal one. Formulation of M(s) incorporates the time-domain characteristics, and the optimal interaction desired to be present in the designed closed-loop system. The developed controller design procedure also works with a user-specified M(s). In the first stage of the controller design, a higher-order controller K(s) which makes the closed-loop system exactly equal to the M(s) is obtained. In the second stage, K(s) is approximated to a FOC or an integer-order (IO) controller (IOC) C(s) with the aim of matching a certain number of approximate generalized time moments (AGTMs) and/or approximate generalized Markov parameters (AGMPs) of K(s) to those of C(s) at a set of frequency points in the s-plane. The simulation and experimental validation of the proposed approach are performed by the design and implementation of the controller for an IO MIMO plant with time-delays. The controller design algorithm is also illustrated based on the user-defined reference model for a FO MIMO plant with time-delays taken from the literature. The obtained results show that the FOC results in better performance compared with its IO counterpart.

INDEX TERMS AGTM and AGMP matching, fractional-order controller, MIMO, model-matching, reference model.

I. INTRODUCTION

Fractional calculus is a generalization of ordinary differentiation and integration to arbitrary (non-integer) order. Field of research on fractional calculus is beyond 300 years old. In the initial period of the research, there were only a few mathematicians and theoretical physicists who were working in this field. However, situations have considerably changed in the last three decades. The main reason behind the growing interest was the applications of fractional calculus in engineering, especially control engineering. Fractional-order (FO) system are best in representing the memory and hereditary properties compared with the integer-order (IO) system [1]. These properties of FO controller (FOC) were exploited to improve the performance of a multi-band power system stabilizer against system uncertainties [2]. Techniques developed by the research community for obtaining the solution of non-integer differential equations over past decades have considerably extended its applications, especially in the areas of system modeling and controller design [3].

The linear quadratic regulator (LQR) design procedure has been widely utilized in the field of control engineering. Two reasons justifying the choice of LQR for solving control problem are: Firstly, it usually leads to a closed-form solution for a given control problem. Secondly, it has an efficient mathematical formulation [3]. The performance of trial and error based manual tuning of weighting matrices of LQR heavily relies on the experience and knowledge of the designer.

The associate editor coordinating the review of this manuscript and approving it for publication was Jie Tang.

Methods based on pole placement [4], genetic algorithm [5], and particle swarm algorithm [6] had been utilized for determining the weighting matrices of the LQR based controller. Methods for determining weighting matrices described in the literature have not considered the interactions present in multiple-input multiple-output (MIMO) systems.

The model-matching technique has been a powerful methodology for controller design of MIMO systems [7]–[10]. The reference model selection in the literature of the model-matching based techniques focuses only on embodying the desired time-domain characteristics of output. A method based on the preservation of pole-zero excess of a plant had been utilized for the selection of a reference model in the model-matching based controller design technique presented in [7]. The reference model selection procedure presented in [8] incorporates specified time-domain specifications. Besides, the method presented in [8] embodied specified interaction to the off-diagonal elements of the transfer function matrix (TFM) of the reference model. The authors of [9] had suggested the idea of a time-varying type reference model which adapts the deviation in the mathematical representation of the plant but had not considered the incorporation of optimal interaction in the reference model. The amount of time-delay that has to be present in a chosen reference model, during the realizable controller design for delayed MIMO plant was addressed in [10]. The FOC design for MIMO systems using the model-matching techniques has not been reported in the literature to the best knowledge of the authors.

Application of FO calculus into controller design field was first introduced in [11]. The superior performance of non-integer order control over the conventional IO proportional-integral-derivative (IOPID) controller was described in [11]. The concept of FOPID controller, introduced in [12], had made a huge impact in control engineering. The method presented in [12] applies to linear systems only. Preliminaries of fractional calculus theory and its valuable applications in the area of control systems were presented in [12]–[14]. The adaptive fuzzy backstepping controller design presented in [13] relies on the approximated fuzzy model of the nonlinear function. It was shown that iso-damping characteristics were possible only with the use of FOC [15], [16]. A model-matching FOC design for single-input single-output (SISO) systems was presented in [17]. For a MIMO IO system, model-matching techniques were used to solve several control problems: design the controller for stable [7] and unstable [18] plants, design of robust decentralized controllers for stable and non-minimum phase plants [19], controller design for disturbance rejection [20], and development of a damping-based controller design framework [21]. The controller design for MIMO FO plants is a growing field of research. The controllers for the FO MIMO plant was designed using the parameter optimization algorithm in [22]. The assessment of robustness of the controller to parametric variations was presented in [2], [11], [16], [19], [22]–[24]. The disturbance rejection capability of the designed controller was investigated in [24]. In [23], the tuning of parameters of FOPD controller for FO plants was considered, which takes advantage of the extra degree of freedom present in the FOC to design a more effective controller. The FOPID controller provided a more flexible tuning strategy in [25]–[27], thereby achieving the control requirement in a better way compared with its IO counterpart. The comparison of the performance of the FOPID controller with the IOPID controller was presented in [25]–[27]. The FOC design for stable and unstable MIMO plants was achieved in [28]. However, work presented in [28] requires pre-decoupling as an initial stage of the FOC design. Matching algorithms based on approximate generalized time moments (AGTMs) [29] and approximate generalized Markov parameters (AGMPs) [30] have been utilized for the rational approximation of MIMO FO system [31]. The work presented in [31] was restricted only to the rational approximation of the FO system by an IO system, where open-loop stability was one of the objectives. In addition, the search space for optimal frequency points was limited to positive real-axis of the s-plane.

An ideal controller, which exactly matches the response of the designed closed-loop system with that of the reference model was synthesized during the controller design technique described for SISO systems in [32]. The ideal controller TFM usually consists of improper or higher-order elements, which leads to difficulties in its practical implementation. Literature such as [32] presented the possibility of finding a reduced IO approximation of the ideal controller with the objective of matching the response of the designed closed-loop system with that of the desired one. A frequency-domain design method for IOPID controller based on the synthesis equation was presented in [33], [34]. The reference model selection and/or controller design procedure presented in [32]–[34] were not generalized one and depended on the designer's knowledge. Suboptimal control of FO systems was presented in [35]. The work in [35] was limited to parametric variations in the system. Work presented in [36] depends on cancellation of non-dominant poles and zeros present in higher-order controller TFM in their design process, leading to a reduced-order implementable controller structure. However, in a practical scenario, pole-zero cancellation will be very difficult to be realized.

The following are major underlying motivations for conducting this research work. Most of the FOC design algorithms presented in the literature such as [2], [12], [17], [25], [26] are based on heuristic methods. To the best of authors knowledge, it is still an interesting and challenging work to develop an algebraic approach for the design of FOC/IOC for a general class of linear time-invariant systems described earlier. The limitation of the reference model selection approaches presented in the literature [7]–[10] is that they do not include information about the plant dynamics. Thereby the feasibility of achieving the objective lies heavily on the knowledge of the designer about the plant. Hence, the selection of a reference model, which takes into account the complete information regarding the

IO/FO plant is still very challenging. Most of the MIMO controller design algorithms presented in the literature such as [7], [10], [19], [22], and [28] yields different denominator polynomials for each element of the controller TFM. These approaches thereby increase the resultant order of the MIMO system. The increase in the order of system increases complexity in its realization. Hence it is advantageous to propose a MIMO FOC design technique, which yields a common denominator polynomial for the controller TFM.

Motivated by the above discussions, this paper investigates the problem of designing a MIMO FOC/ IO controller (IOC), by solving a set of simultaneous linear algebraic equations for a given set of fractional/integer exponents of the numerator and denominator polynomials of each element of the controller TFM. It also investigates the possibility of a generalized reference model selection procedure, applicable for both IO and FO linear systems. The present work provides some solutions to the problems identified in the literature. The main contributions of this work are as follows: (1) A novel streamlined procedure for the selection of a reference model in the design of the model-matching suboptimal FOC/IOC is presented. The incorporation of finding an optimal interaction for a given time-domain specification is one of the key features of the reference model selection procedure in the proposed work. Also, the reference model is formulated by considering the dynamics of the plant. The proposed reference model selection procedure is based on the LQR with integral action (LQRI). (2) The proposed algorithm can be said to provide a generalized algebraic method, to determine the coefficients of numerator and denominator of each element of MIMO FOC/IOC with the objective of meeting the desired closed-loop specification. The FOC/IOC design is achieved using the AGTM/AGMP matching method, ensuring the closed-loop system stability. The algorithm gives out a unique search strategy which involves the two-dimensional space in the s-plane in pursuit of the optimal frequency points. The desired frequency band of approximation decides the bounds for each frequency variables. Pre-decoupling is not required in the proposed controller design method. (3) The proposed method yields a MIMO FOC/IOC with a common denominator in each element of the controller TFM. The advantage of the controller design technique is that it yields a low order controller of predefined/optimal order and the controller structure need not be fixed. The user can choose any controller structure to achieve the objectives. Certain controller parameters can be chosen, and the remaining can be obtained according to the developed algorithm, resulting in a reduction in hardware compulsion. (4) The proposed FOC/IOC design procedure ensures the steady-state matching (SSM) of the designed closed-loop system to that of the reference model.

The paper is organized as follows. Section II gives the preliminary definitions of fractional derivative operator. Section III describes the proposed reference model selection procedure. The controller design methodology is described in Section IV. The proposed controller design methodology is applied to two plants: an IO MIMO plant with time-delays [8] and a FO MIMO plant with time-delays [22]. The simulation and experimental results are summarized in Section V and Section VI, respectively. Finally, the conclusions and future scope are presented in Section VII.

II. DEFINITIONS OF FRACTIONAL DERIVATIVE OPERATOR

The definitions of the noninteger-order derivative operator are summarised in this section. The most widely used definitions of non-integer order derivatives fall into three main categories: the Riemann-Liouville definition, the Caputo definition and the Grünwald-Letnikov definition [3]. The definitions by Riemann-Liouville and Grünwald-Letnikov are equivalent. The Riemann-Liouville definition is given by

$$\frac{d^{\alpha}}{dt^{\alpha}}x(t) \equiv D^{\alpha}x(t) = \frac{d^{n}}{dt^{n}}\left[\frac{1}{\Gamma(n-\alpha)}\int_{0}^{t}(t-\tau)^{n-\alpha-1}x(\tau)d\tau\right], \quad (1)$$

where $\alpha \in \Re^{+}$, $n-1 < \alpha < n$, $n \in \mathbb{N}$ and $\Gamma(\cdot)$ is the Gamma function.

The Caputo definition is defined as

$$\frac{d^{\alpha}}{dt^{\alpha}}x(t) = \frac{1}{\Gamma(n-\alpha)}\int_{0}^{t}(t-\tau)^{n-\alpha-1}x^{(n)}(\tau)d\tau, \quad (2)$$

where $n-1 < \alpha < n$, $n \in \mathbb{N}$.

III. GENERALIZED REFERENCE MODEL SELECTION

In this section, a streamlined procedure for the selection of a reference model to be used in the model-matching techniques is presented. The developed procedure applies to plant having either integer or fractional dynamic representation. If a plant has IO dynamics, then the reference model obtained will be of IO. If the plant possesses FO representation, then the reference model obtained will be of FO.

The developed method proposes a generalized LQRI-based closed-loop system (GLCLS) model as $M(s)$. The reference model selection procedure focuses on obtaining the optimal interaction factor for given desired output time-domain specifications. In addition, the GLCLS design procedure determines the optimum main diagonal elements of the diagonal weighting matrices Q and R. As a first step in the formulation of the GLCLS model, a generalized initial model (GIM) is framed with the desired time-domain specifications. The interaction parameters of the GIM are kept as tuning parameters. The GLCLS model is framed by tuning the elements of the weighting matrices in the optimal state feedback design procedure. The interaction thus developed in the GLCLS model is mapped onto the GIM by tuning the interaction parameters. The desired time-domain specifications of the GIM are used to tune the elements of the weighting matrices of the GLCLS model. Thus, GLCLS model reflects the

desired time-domain specifications and the optimal interaction to be present in the designed-closed loop system.

Let, the mathematical representation of a multivariable LTI FO system [3] be

$$D^{\alpha}x = Ax + Bu, \tag{3}$$

$$y = Cx + Hu, \tag{4}$$

where $\alpha = [\alpha_1 \alpha_2 \ldots \alpha_n]$, $u \in \Re^{q\times 1}$ is the input vector [14], $x \in \Re^{n\times 1}$ is the state vector, $y \in \Re^{p\times 1}$ is the output vector, $A \in \Re^{n\times n}$ is the state matrix, $B \in \Re^{n\times q}$ is the input matrix, $C \in \Re^{p\times n}$ is the output matrix, and $H \in \Re^{p\times q}$ is the direct transmission matrix, respectively. The TFM representation of the system, presented in (3) and (4), is:

$$P(s) = C\left\{(s^{\alpha}I - A)^{-1}B\right\} + H. \tag{5}$$

The system presented in (5) represents an IO system if all the elements of α-vector i.e. α_i's are unity.

A. GIM

The GIM is framed from the desired closed-loop specifications such as settling time, rise time, damping ratio, etc. An IO or FO representation can be used to represent the dynamics of the GIM. The response of the GIM in the s-domain, for an input vector $R(s) = [R^{(k,1)}(s)]$, can be expressed as:

$$\left[Y_m^{(i,1)}(s)\right] = \left[G_m^{(i,k)}(s)\right]\left[R^{(k,1)}(s)\right], \tag{6}$$

where $G_m^{(i,k)}(s)$, $i = 1, 2, \ldots, p$; $k = 1, 2, \ldots, q$ represents an element of the GIM TFM relating the ith output to the kth input. Consider the case where the input vector to the system consists of step signals with amplitude D_k. In the present work, a three-term FO low-pass filter structure presented in [37] has been utilized to represent the dynamics of $Y_m^{(i,1)}(s)$. The ith response $Y_m^{(i,1)}(s)$ of the GIM due to kth input is taken in the form of a step response of a generalized three-term low-pass filter as

$$Y_m^{(i,1)}(s) = \frac{\mathrm{D_k}\omega_n^2}{s(s^{2\alpha} + 2\zeta\omega_n s^{\alpha} + \omega_n^2)}, \tag{7}$$

where $\alpha \in \Re^{+}$ is the base order. The desired closed-loop time-domain specifications such as natural frequency ω_n, damping ratio ζ, etc., can be embodied to an IO representation using the work presented in [8] and to a FO representation using the work presented in [37]. In the present work, the off-diagonal elements of the GIM TFM have been taken in the form of an αth order two-term FO system with zeros taken at infinity. The diagonal elements of the GIM are then obtained as

$$G_m^{(u,u)}(s) = \frac{\left(sY_m^{(u,1)}(s) - \sum_{\substack{\forall k \\ k\neq u}} \frac{D_k}{(s^{\alpha}+\lambda^{(u,k)})}\right)}{D_u}, \tag{8}$$

where $\lambda^{(u,k)}$ represents the interaction to be present in the designed closed-loop system, $u = 1, 2, \ldots, min(p,q)$; $k = 1, 2, \ldots, q$. Hence, for a given desired time-domain specification, the dynamics of $G_m(s)$ will be a function of the parameter $\lambda^{(u,k)}$. The value of $\lambda^{(u,k)}$ quantifies the level of interaction that can be present in the controlled dynamics. Higher values of $\lambda^{(u,k)}$ imply a system with lesser interactions and vice versa. Interaction present in a MIMO plant makes its control more challenging.

B. GLCLS MODEL

The GLCLS model includes an integrating action along with full state feedback optimal controller. The combined structure is as given in [38]. The difference between input and output vectors are integrated, and the outputs of the integrators are considered as additional states. GLCLS model TFM representation can be obtained by

$$M(s) = C_{ag}(s^{\alpha}I_{(n+p)} - (A_{ag} - B_{ag}K_{op}))^{-1}E, \tag{9}$$

where $K_{op} = -\begin{bmatrix} K & K_i \end{bmatrix}$, $K_{op} \in \Re^{q\times(n+p)}$, $A_{ag} = \begin{bmatrix} A & O_{n\times p} \\ -C & O_{p\times p} \end{bmatrix}$, $B_{ag} = \begin{bmatrix} B \\ O_{p\times q} \end{bmatrix}$, $C_{ag} = \begin{bmatrix} C & O_{p\times p} \end{bmatrix}$, and $E = \begin{bmatrix} O_{n\times p} \\ I_p \end{bmatrix}$. Here, O represents the null matrix, the subscript of which indicates its dimension. The constant matrices $K \in \Re^{q\times n}$ and $K_i \in \Re^{q\times p}$ are the state feedback gain and integral gain matrices, respectively. In the present work, the weighting matrix S in the cost function of the conventional LQR problem is set as zero. The optimal state-feedback gain matrix K_{op} is thereby obtained by solving the following algebraic Riccati equation for a given set of values of weighting matrices Q and R [39]:

$$A^T P + PA - PBR^{-1}B^T P + Q = 0, \tag{10}$$

where P is the solution of the algebraic Riccati equation, and the superscript T denotes the transpose of the matrix. From (9), it can be seen that the formulation of the GLCLS model involves information about plant dynamics.

In the present work, the problem of finding the elements of the weighting matrices has been framed in an optimization setup. The optimization framework is formed with the objective of matching the step response of the GLCLS model with that of the GIM and can be stated as follows:

Find (i) $\lambda^{(u,k)}$ (ii) α (in case of FO GIM), and (iii) elements of the state and input weighting matrices of the GLCLS model, to

$$\begin{cases} \text{minimize } J_1 = \int_0^{t_f} \left(y_m^{(i,k)}(t) - y_d^{(i,k)}(t)\right)^2 dt \\ \text{subject to } \begin{cases} \text{(i) State weighting matrix } Q \text{ should be} \\ \text{symmetric positive semidefinite} \\ (Q \succeq 0) \text{ i.e. } x^T(t)Qx(t) \geq 0,\ \forall\, x(t) \neq 0 \text{ and} \\ \text{(ii) Input weighting matrix } R \text{ should be} \\ \text{symmetric positive definite matrix} \\ (R \succ 0) \text{ i.e. } u^T(t)Ru(t) > 0,\ \forall\, u(t) \neq 0, \end{cases} \end{cases} \tag{11}$$

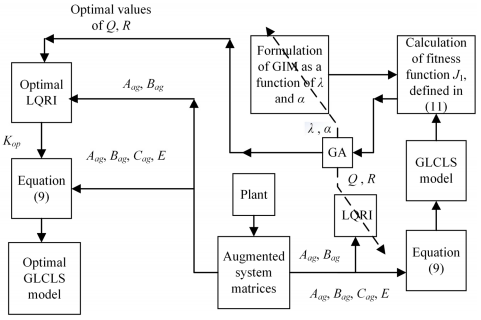

FIGURE 1. Flow diagram of the proposed reference model selection procedure.

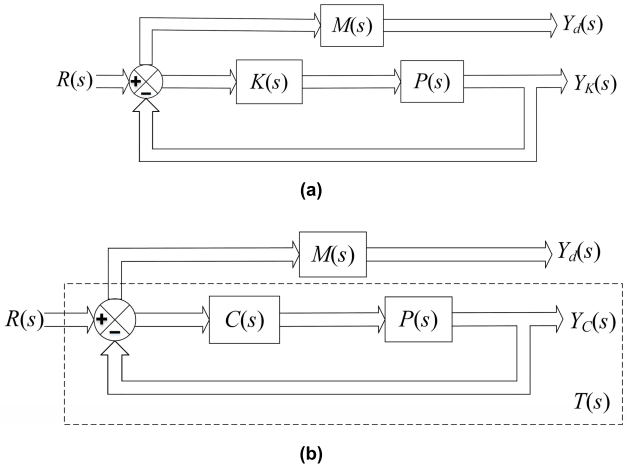

FIGURE 2. Block diagram of the controller design algorithm. (a) First stage. (b) Second stage.

where $y_m^{(i,k)}(t)$ and $y_d^{(i,k)}(t)$ represents the step responses of transfer functions relating the ith output to the kth input of $G_m(s)$ and $M(s)$, respectively. The vector of state variables and input variables are represented by $x(t)$ and $u(t)$, respectively. If the desired time-domain specifications of the designed closed-loop system are feasible, the solution of (11) always exist. The reference model is formed by substituting the optimal values of the decision variables $\lambda^{(u,k)}$, α, and the elements of the weighting matrices into (9). The objective function presented in (11) ensures that the GLCLS model embodies the desired time-domain specifications. The overall procedure for obtaining the optimal GLCLS model can be illustrated in the form of a flow diagram as shown in Fig. 1.

The selection of the GLCLS model as the reference model tackles the difficulty in embodying the required interaction that has to be present in the controlled dynamics. Besides, the GLCLS model design procedure demands the need for imparting the desired specifications to the weighting matrices of the LQRI. In this work, both of these problems have been tackled with the help of a properly framed optimization procedure. The selection of the GLCLS model over the GIM as an input to the first stage of the proposed model-matching-based controller design procedure guarantees two major advantages. First, the GLCLS model is formulated by considering the dynamics of the plant. Second, the GLCLS model is designed to contain the desired/optimal interaction to be present in the controlled dynamics for a given set of desired specifications. The performance of the designed closed-loop system mimics that of the GLCLS model. Since the GLCLS model is designed using optimal control theory, the designed output-feedback closed-loop system can be termed as a suboptimal one.

IV. PROPOSED CONTROLLER DESIGN SCHEME

In this section, the methodology for the model-matching FOC/IOC design is presented. Block diagrams of the first and second stages of the two-stage controller design algorithm have been shown in Figs. 2(a) and 2(b), respectively. The objective is to design a MIMO FOC/IOC $C(s)$ for a MIMO plant $P(s)$ with the aim of making the response of the designed closed-loop system $Y_C(s)$ as close as possible to the desired characteristics $Y_d(s)$. The desired specifications are embodied in the reference model $M(s)$. The designed closed-loop system $T(s)$ is a unity feedback system consisting of the plant and the controller in the forward path and is shown within dashed lines in Fig. 2(b).

In the first stage, a higher-order ideal controller TFM $K(s)$ is obtained from the plant and the reference model TFMs. The rational approximation in the second stage is achieved by matching a few numbers of AGTMs/AGMPs of $K(s)$ to those of low-order controller $C(s)$ at a set of frequency points in the s-plane. The AGTMs/AGMPs matching is utilized to form a set of non-homogeneous simultaneous equations. The solution of these set of equations gives the values of numerator and denominator coefficients in each element of $C(s)$.

The analytical expression for the ideal controller $K(s)$ which makes the closed-loop system exactly equal to the $M(s)$ can be obtained as:

$$K(s) = P(s)^{-1}M(s)(I - M(s)). \tag{12}$$

Equation (12) yields a TFM which is practically difficult to implement due to its improper or higher-order dynamics. Let $C(s) = [C^{(i,k}(s)]$. Each element of the $C(s)$ can be represented by a general structure $n + 1$ term FO transfer function as follows:

$$C^{(i,k)}(s) = \frac{c_0^{(i,k)} + c_1^{(i,k)}s^{\beta_1^{(i,k)}} + \ldots + c_{m^{(i,k)}}^{(i,k)}s^{\beta_{m^{(i,k)}}^{(i,k)}}}{d_0 + d_1 s^{\alpha_1} + \ldots + d_{n-1}s^{\alpha_{n-1}} + s^{\alpha_n}}, \tag{13}$$

where $u - 1 < \beta_u^{(i,k)} \leq u$ and $v - 1 < \alpha_v \leq v$ with $u = 1, 2, \ldots, m^{(i,k)}$ and $v = 1, 2, \ldots, n$. Assigning values to α_v and $\beta_u^{(i,k)}$ as α_v^* and $\beta_u^{*(i,k)}$, respectively, satisfying the above-specified range, the parameters d's and $c^{(i,k)}$'s of (13) becomes the unknown parameters of $C^{(i,k)}(s)$, which are to be determined with the objective of making the performance of $C(s)$ as close as possible with that of $K(s)$. The total number of unknown coefficients d's and $c^{(i,k)}$'s for each element of

the controller TFM presented in (13) can be obtained as $n + \left(m^{(i,k)} + 1\right)$. Hence the total number of unknown coefficients of the $p \times q$ MIMO controller n_u is obtained by

$$n_u = n + \sum_{i=1}^{p} \sum_{k=1}^{q} \left[\left(m^{(i,k)} + 1\right)\right]. \tag{14}$$

The objective is to obtain the unknown parameters of the FOC/IOC $C(s)$ such that n_w number of AGTMs and/or AGMPs of higher-order controller matches to those of its approximant, i.e.,

$$C(s)|_{s=\delta_r} = K(s)|_{s=\delta_r}, \tag{15}$$

where δ_r, $r = 1, 2, \ldots, n_w$ are frequency points in the s-plane, and n_w is the minimum number of the frequency points to be chosen, in the desired frequency band of approximation. The minimum number of frequency points can be obtained using ceiling function as

$$n_w = \lceil n_u/(pq) \rceil. \tag{16}$$

The total frequency points across the s-plane n_w consist of frequency points along the real axis n_x, frequency points along the imaginary axis n_y, and complex frequency points having both real and imaginary parts n_c, i.e.,

$$n_w = n_x + n_y + n_c. \tag{17}$$

Hence, each of the n_w frequency points can be either of the three types: purely real, purely complex or complex with its real part not equal to zero.The search process for optimal values of expansion points is carried out along with those of the distribution of frequency points n_x, n_y,and n_c across the s-plane, in an optimization framework as presented in the section IV-A. Equation (12) is utilized for determining the right-hand side of (15). Let $(i, k)th$ element of matrix present in the right-hand side of (15) be represented by $f_r^{(i,k)}$, where $i = 1, 2, \ldots, p$ and $k = 1, 2, \ldots, q$. Then,

$$C(s)|_{s=\delta_r} = \left[f_r^{(i,k)}\right]. \tag{18}$$

Equating the corresponding elements on both sides of (18) lead to

$$\frac{c_0^{(i,k)} + c_1^{(i,k)} (\delta_r)^{\beta_1^{(i,k)}} + \ldots + c_{m^{(i,k)}}^{(i,k)} (\delta_r)^{\beta_{m^{(i,k)}}^{(i,k)}}}{d_0 + d_1 (\delta_r)^{\alpha_1} + \ldots + d_{n-1} (\delta_r)^{\alpha_{n-1}} + (\delta_r)^{\alpha_n}} = f_r^{(i,k)}. \tag{19}$$

Cross-multiplying and equating the coefficients of like terms, a set of nonhomogeneous simultaneous equations are constructed as

$$A_r^{(i,k)} X^{(i,k)} = B_r^{(i,k)}, \tag{20}$$

where

$$X^{(i,k)} = [X_c^{(i,k)} \; X_d]^T, \tag{21}$$

with

$$X_c^{(i,k)} = \left[c_{m^{(i,k)}}^{(i,k)} \; c_{(m^{(i,k)}-1)}^{(i,k)} \; \cdots \; c_1^{(i,k)} \; c_0^{(i,k)}\right], \tag{22}$$

and

$$X_d = [d_{n-1} \; d_{n-2} \; \ldots \; d_0]. \tag{23}$$

The matrices $A_r^{(i,k)}$ and $B_r^{(i,k)}$ are constructed as

$$A_r^{(i,k)} = [S_c^{(i,k)} \; -f_r^{(i,k)} S_d]\Big|_{s=\delta_r}, \tag{24}$$

$$B_r^{(i,k)} = f_r^{(i,k)} \times \delta_r^{\alpha_n}, \tag{25}$$

where

$$S_c^{(i,k)} = \left[(s)^{\beta_{m^{(i,k)}}^{(i,k)}} \; (s)^{\beta_{m^{(i,k)}-1}^{(i,k)}} \; \ldots \; (s)^{\beta_1^{(i,k)}} \; 1\right], \tag{26}$$

and

$$S_d = \left[(s)^{\alpha_{n-1}} \; (s)^{\alpha_{n-2}} \; \ldots \; (s)^{\alpha_1} \; 1\right]. \tag{27}$$

For each frequency point δ_r, (20) leads to the formation of the $p \times q$ set of equations. These set of matrix equations can be cascaded in the form of:

$$A_r X = B_r, \tag{28}$$

where

$$X = [X_c^{(1,1)} \; X_c^{(1,2)} \; \ldots \; X_c^{(1,q)} \; X_c^{(2,1)} \; X_c^{(2,2)} \ldots \; X_c^{(2,q)} \ldots \; X_c^{(p,1)} \; X_c^{(p,2)} \ldots \; X_c^{(p,q)} \; X_d]^T, \tag{29}$$

A_r is obtained as shown in (30), as shown at the top of the next page, where $O_{1\times(m^{(i,k)}+1)}$ represents the null matrix of dimension $1 \times (m^{(i,k)} + 1)$.

$$B_r = \left[f_r^{(1,1)} \; f_r^{(1,2)} \ldots f_r^{(1,q)} f_r^{(2,1)} \; f_r^{(2,2)} \ldots \; f_r^{(2,q)} \ldots f_r^{(p,1)} f_r^{(p,2)} \ldots f_r^{(p,q)}\right]^T \times \left(\delta_r^{\alpha_n}\right). \tag{31}$$

Matrices A_r and B_r, obtained at each frequency point are cascaded to form the resultant matrices A and B, respectively. This cascading leads to a set of non-homogeneous equations in the form:

$$AX = B. \tag{32}$$

The least squares solution of (32) yields values of the unknown parameters in vector X, given in (29), (22), and (23), thereby obtaining the numerator and denominator coefficients in each element of $C(s)$. Equation (32) is also utilized to match the steady-state response of the designed-closed-loop system with that of the reference model as presented in section IV-B. The procedure presented in this section for obtaining the numerator and denominator coefficients in each element of $C(s)$ is for one set of decision variables, which are n_x,n_y,n_c, δ_r, α_v^*, and $\beta_u^{*(i,k)}$.

$$A_r = \begin{bmatrix} S_c^{(1,1)} & O_{1\times(m^{(1,1)}+1)} & O_{1\times(m^{(1,1)}+1)} & O_{1\times(m^{(1,1)}+1)} & \cdots & \cdots & -f_r^{(1,1)}S_d \\ O_{1\times(m^{(1,2)}+1)} & S_c^{(1,2)} & O_{1\times(m^{(1,2)}+1)} & O_{1\times(m^{(1,2)}+1)} & \cdots & \cdots & -f_r^{(1,2)}S_d \\ \vdots & \vdots & \ddots & \vdots & \vdots & \vdots & \vdots \\ O_{1\times(m^{(p,q)}+1)} & O_{1\times(m^{(p,q)}+1)} & O_{1\times(m^{(p,q)}+1)} & O_{1\times(m^{(p,q)}+1)} & \cdots & S_c^{(p,q)} & -f_r^{(p,q)}S_d \end{bmatrix}, \tag{30}$$

A. SELECTION OF OPTIMAL DECISION VARIABLES

The objective function for choosing the optimal decision variables has been chosen as the integral of squared deviations in the step response of the designed closed-loop system from that of the reference model over a chosen simulation time. The distribution of frequency points across the s-plane n_x, n_y, and n_c influences the performance of the proposed approximation method. The proposed method, therefore, determines the optimum values of frequency points along with its optimum distribution across the s-plane. Hence the decision variables v is the set of frequency variables δ_r along with their distribution n_x, n_y, and n_c in the s-plane. The problem of finding optimal values of n_w frequency points and those of the fractional exponents of the numerator and denominator polynomials of each element of the $C(s)$ is framed in an optimization framework. The optimization framework can be stated as follows:

Find (i) n_x,n_y,n_c (ii) δ_r (iii) α_v^*, and (iv) $\beta_u^{*(i,k)}$, to

$$\begin{cases} \text{minimize } J_2 = \int_0^{t_f} \left(y_d^{(i,k)}(t) - y_c^{(i,k)}(t)\right)^2 dt \\ \text{subject to} \begin{cases} (i)\, u - 1 < \beta_u^{(i,k)} \leq u \\ (ii)\, v - 1 < \alpha_v \leq v \\ (iii)\, \text{The poles of } T(s) \text{ should be} \\ \qquad \text{in the left-half of the } s\text{-plane,} \end{cases} \end{cases} \tag{33}$$

where $y_d^{(i,k)}(t)$ and $y_c^{(i,k)}(t)$ represents the step responses of transfer functions relating the ith output to the kth input of $M(s)$ and $T(s)$, respectively; t_f is the total simulation time.

B. CLOSED-LOOP SYSTEM SSM

In this work, a provision has been incorporated for matching the steady-state response of the designed-closed loop system with that of the reference model. The SSM can be incorporated using the final-value theorem:

$$\lim_{s\to 0} sY_c(s) = \lim_{s\to 0} sY_d(s). \tag{34}$$

Equation (34) in the case of a unit-step input takes the form:

$$\lim_{s\to 0} T(s) = \lim_{s\to 0} M(s), \tag{35}$$

$$\lim_{s\to 0} [I + P(s)C(s)]^{-1} P(s)C(s) = \lim_{s\to 0} M(s), \tag{36}$$

$$\lim_{s\to 0} C(s) = \lim_{s\to 0} P^{-1}(s)M(s)(I - M(s))^{-1}. \tag{37}$$

Substituting the structure of the controller (13) in (37) yields

$$c_0^{(i,k)} \Big/ d_o = \lim_{s\to 0} P^{-1}(s)M(s)(I - M(s))^{-1}. \tag{38}$$

The matching of the steady-state response of the reference model with that of the designed closed-loop system is achieved by using (38) in (32). By adopting this scheme of SSM, the number of parameters in $C(s)$ get reduced by the product of p and q for a $p \times q$ MIMO system. The SSM algorithm is valid if the respective limits in (37) exist.

V. SIMULATION RESULTS

This section illustrates the application of the proposed algorithm first to a linear MIMO IO plant and then to a linear MIMO FO plant, both with time-delay characteristics. The comparative results of the simulation of the designed closed-loop system with that of the reference model are presented. The design of FOCs and IOCs have been accomplished using the same algorithm to have a basis for comparison. The effectiveness and robustness of the proposed controller design strategy are assessed using linear time-domain simulations.

In this work, because of the first two constraints presented in (33), the values of $m^{(i,k)}$ have been taken one less than that of n ($m^{(i,k)} = n - 1$), to ensure that the elements of the designed $C(s)$ in (13) are strictly proper. In addition, the variable n is allowed to take the values two or three which results in the three-term and four-term controller, respectively. Using the same procedure, keeping the base order as unity, IOC is also designed. The FO three-term, four-term and PID structure controllers along with their IO counterpart have been designed using the proposed method. The design of PID structures has been carried out by incorporating a low-pass filter along with the differentiator. In this work, the fundamental sample time and the total simulation time t_f for the evaluation of the integral squared error (ISE) index presented in (33) have been taken as 0.1 s and 15 s, respectively. The desired frequency band of approximation has been taken as (10^{-5}-10^{2}) rad/s.

A. MIMO IO PLANT WITH TIME-DELAYS

The proposed controller design strategy has been illustrated by designing a velocity controller for a two-wheeled mobile robot (Quanser QBot 2) taken from the literature. The mathematical representation of the wheeled mobile robot is described in [8]. During the Hardware-in-the-Loop simulation of the wheeled mobile robot, a time-delay of 1.4 s and a reduction by a factor of 0.9225 in the steady-state value was

observed in the open-loop wheel velocity profiles. Sample time used in the real-time system, delay in actuator dynamics, and friction may have contributed to the undesirable characteristics in the velocity profiles during Hardware-in-the-Loop simulation. The delay and steady-state error observed in the velocity profiles are compensated in the mathematical representation of wheeled mobile robot dynamics as

$$P(s) = \tilde{P}(s) \times 0.9225 \times e^{-1.4s}, \tag{39}$$

where $\tilde{P}(s)$ is the TFM representation of the plant obtained in [8].

1) REFERENCE MODEL

The transport delay observed during the Hardware-in-the-Loop simulation of the wheeled mobile robot is also considered in the formulation of the reference model. Hence the transport delay of each element of the reference model TFM has been taken as 1.4 s. Since the plant is modeled in a classical way, the obtained GLCLS model is of IO. The proposed reference model can be selected in two different ways: one by taking the GIM as an IO representation, and one by considering it as a FO one. In this work, the fundamental sample time and the total simulation time t_f for the evaluation of the ISE index presented in (11) have been taken as 0.01 s and 10 s, respectively. The optimal values of the parameters of the GIM and the GLCLS model are determined by using the procedure presented in section III and are given in the appendix.

Case 1: IO GIM

In the case of IO GIM, the value of α in (7) and (8) has been taken as unity. The settling time and damping ratio of the desired response are chosen as 3 s and 1.1, respectively. The steady-state value of the right wheel velocity D_1 has been taken as 0.2 m/s. For a circular trajectory with a radius of 0.35 m, the steady-state value of left wheel velocity D_2 is evaluated as 0.1 m/s [8].

The comparisons of the velocity profiles of the optimal IO GIM with that obtained using the IO GLCLS model are shown in Figs. 3(a)-3(d). It clearly shows that the time-domain specifications of the IO GIM are embodied in the GLCLS model. The GLCLS model is formed with the inclusion of the information of the plant, whereas the GIM is an arbitrary transfer function embodying the desired time-domain specifications. The optimal interaction also gets embodied in the GLCLS model, which is the sufficient interaction required within the GLCLS model to achieve the desired time-domain specifications.

Case 2: FO GIM

The FO GIM takes the form of a three-term FO system, which can be utilized to embody the desired time-domain specifications as presented in [37]. The desired damping ratio has been taken as 0.58. The tolerance fraction for the evaluation of settling time has been taken as 2%. The rest of the time-domain specifications are taken the same as in the IO GIM case. The comparisons of the velocity profiles of the optimal FO GIM to that obtained using the IO GLCLS model

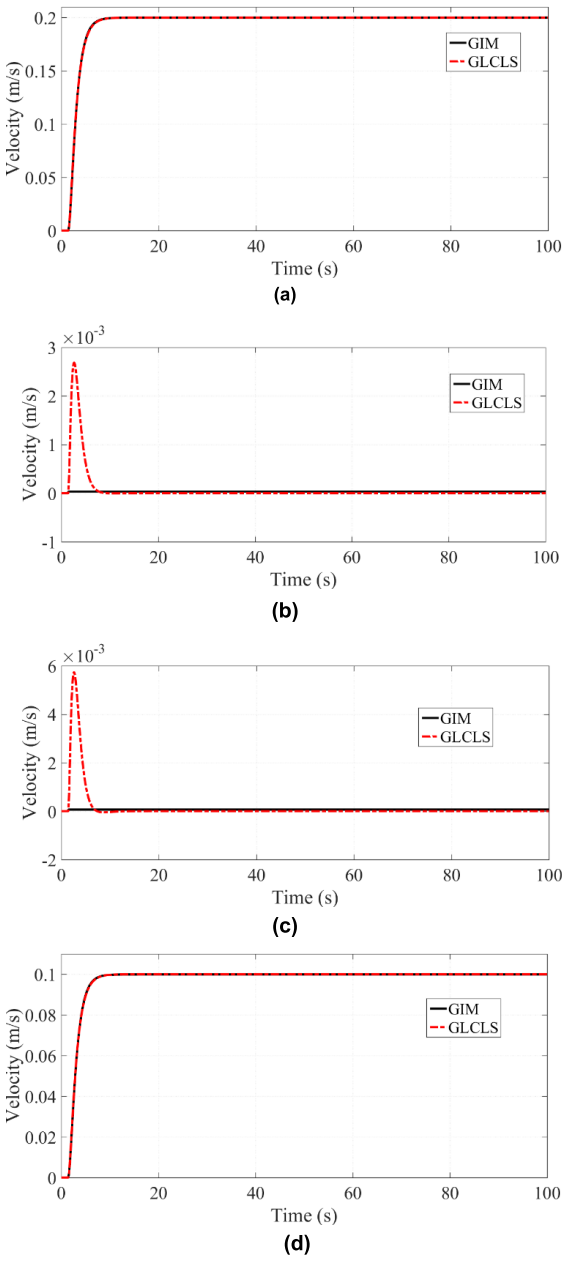

FIGURE 3. Comparison between the velocity profiles of IO GIM and IO GLCLS model at (a) output 1 due to input 1 (b) output 1 due to input 2 (c) output 2 due to input 1 (d) output 2 due to input 2.

are presented in Figs. 4(a)-4(d). It clearly shows that the time-domain specifications of the FO GIM are embodied in the GLCLS model. The response of the off-diagonal elements of the GLCLS model is close to that of the corresponding elements of the GIM with a maximum error of 10^{-3} m/s.

2) PERFORMANCE EVALUATION OF IOC/FOC FOR IO PLANT WITH TIME-DELAYS

The minimum value of the objective function J_2 defined in (33), obtained in the case of IO GIM representation is given in Table 1. The corresponding value for the FO GIM is given in Table 2. The SSM algorithm presented in section IV cannot

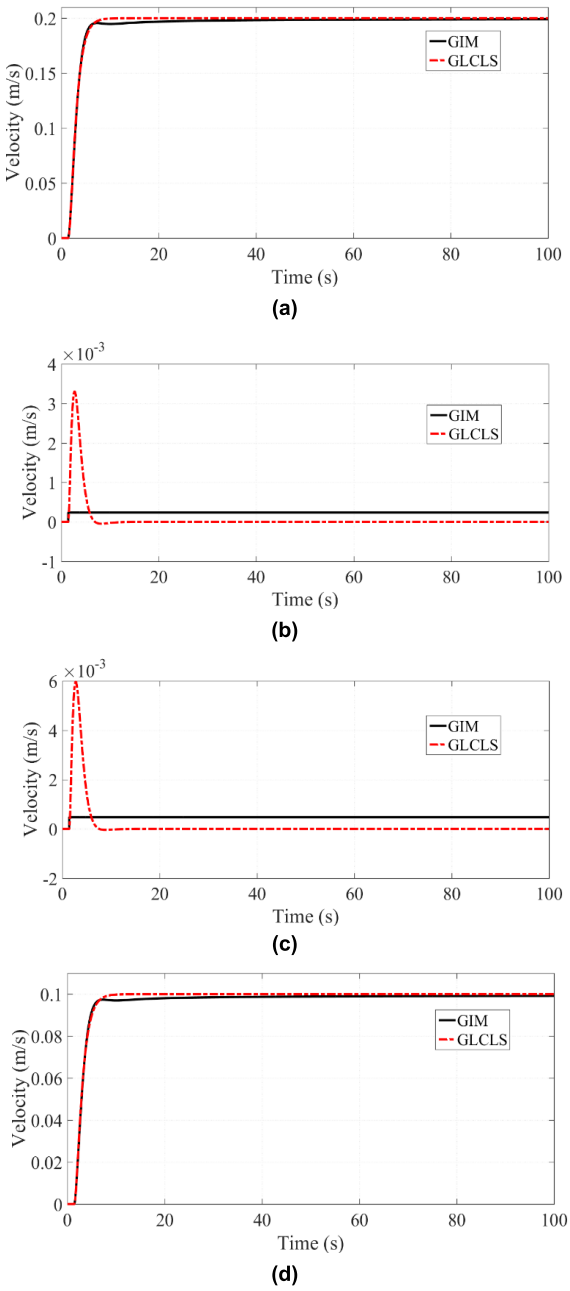

FIGURE 4. Comparison between the velocity profiles of the FO GIM and IO GLCLS model at (a) output 1 due to input 1 (b) output 1 due to input 2 (c) output 2 due to input 1 (d) output 2 due to input 2.

TABLE 1. Minimum value of the objective function J_2 for wheeled mobile robot, keeping IO GIM.

	Without SSM		With SSM	
$C(s)$	IO	FO	IO	FO
3 term	6.74×10^{-4}	5.84×10^{-4}	6.57×10^{-4}	6.04×10^{-4}
4 term	2.26×10^{-5}	1.62×10^{-5}	2.47×10^{-4}	3.32×10^{-5}
PID	0.0025	3.26×10^{-4}	n/a	n/a

be utilized in the case of controllers with PID structure since the left-hand side of (37) becomes infinity for such type of controllers. From Tables 1 and 2, it is clear that FOC achieves better ISE index compared with its IO counterpart.

TABLE 2. Minimum value of the objective function J_2 for wheeled mobile robot, keeping FO GIM.

	Without SSM		With SSM	
$C(s)$	IO	FO	IO	FO
3 term	6.52×10^{-4}	6.45×10^{-4}	8.09×10^{-4}	7.8×10^{-4}
4 term	2.56×10^{-5}	2.06×10^{-5}	4.13×10^{-4}	8.33×10^{-5}
PID	0.0027	4.24×10^{-4}	n/a	n/a

TABLE 3. Minimum value of the objective function J_2 with 100% parametric variation for wheeled mobile robot, keeping IO GIM.

	Without SSM		With SSM	
$C(s)$	IO	FO	IO	FO
3 term	5.14×10^{-4}	5.75×10^{-4}	6.74×10^{-4}	6.10×10^{-4}
4 term	4.88×10^{-5}	6.04×10^{-5}	2.22×10^{-4}	7.24×10^{-5}
PID	0.0024	3.48×10^{-4}	n/a	n/a

TABLE 4. Minimum value of the objective function J_2 with 150% parametric variation for wheeled mobile robot, keeping IO GIM.

	Without SSM		With SSM	
$C(s)$	IO	FO	IO	FO
3 term	7×10^{-4}	5.81×10^{-4}	6.94×10^{-4}	6.16×10^{-4}
4 term	7.68×10^{-5}	9.61×10^{-5}	2.25×10^{-4}	1.03×10^{-4}
PID	0.0024	3.71×10^{-4}	n/a	n/a

From both Table 1 and Table 2, it can be seen that the minimum value of optimum ISE indices is obtained for the four-term FOC, $C(s)$. The corresponding TFMs are shown at the bottom of the next page.

Since there always exists a mismatch between the mathematical model of the plant and the actual plant, the investigation of robustness of the designed controllers to parametric variations is a major concern in every controller design procedures. In the present work, the robustness to parametric variations has been investigated in the simulation. The performance of the designed-closed loop system is analyzed by changing the parameters such as mass, the moment of inertia and the distance between the wheels of the mobile robot, each by 100 % and 150 %. The robustness assessment is carried out by selecting IO representation for the GIM. The minimum value of the objective function J_2 defined in (33), for the abovementioned parameters variations by 100 % and 150 % are given in Table 3 and Table 4 respectively. Comparison between the velocity profiles of the wheeled mobile robot during 150% parametric variation with those of the reference model is shown in Fig. (5). The robustness to parameter uncertainties offered by the proposed controller is evident from Tables 3, 4, and Fig. (5).

B. MIMO FO PLANT WITH TIME-DELAYS

Consider a MIMO FO plant with interaction and time-delay properties between its I/O channels [22]:

$$P(s) = \begin{bmatrix} \dfrac{1}{1.35s^{1.2}+2.3s^{0.9}+1}e^{-0.2s} & \dfrac{2}{4.13s^{0.7}+1}e^{-0.2s} \\ \dfrac{1}{0.52s^{1.5}+2.03s^{0.7}+1} & -\dfrac{1}{3.8s^{0.8}+1}e^{-0.5s} \end{bmatrix}. \quad (40)$$

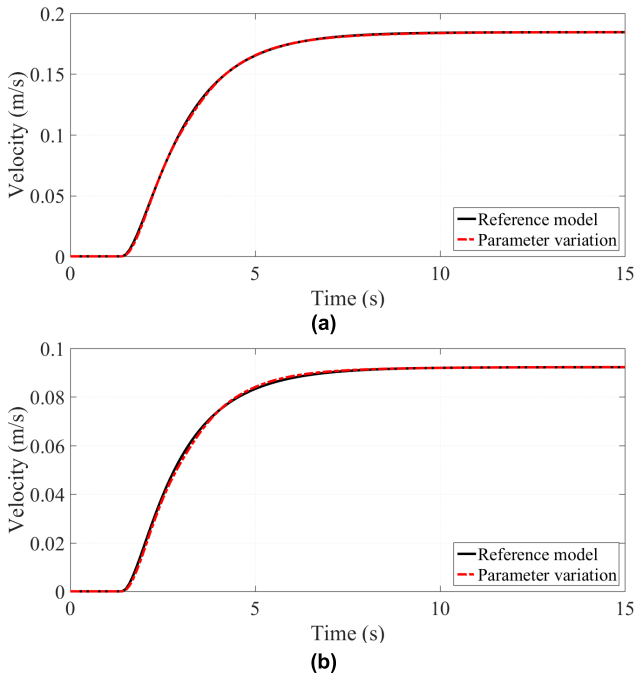

FIGURE 5. Comparison between the velocity profiles of the wheeled mobile robot during 150% parametric variation with those of the reference model. (a) right wheel. (b) left wheel.

The following subsections illustrate the performance of the proposed FOC/IOC design methodology based on a user-defined reference model.

1) USER-DEFINED REFERENCE MODEL

The proposed controller design technique for the FO plant presented in (40) has been carried out by taking two different types of reference models: (i) $M(s)$ as presented in [22], which is of having a dc gain equal to an identity matrix I and (ii) $M(s)$ having a dc gain other than an identity matrix. In the first type of chosen reference model, the designed closed-loop system is expected to behave like a fully decoupled system. However, while incorporating SSM, an identity matrix for the dc gain of the reference model TFM makes the dc gains of $C(s)$ undefined according to (37). Hence, in order to achieve SSM, the second type of the user-defined reference model has been arbitrarily taken as:

$$M(s) = \begin{bmatrix} \dfrac{9}{(s+3)^2} & \dfrac{0.09}{(s+3)^2} \\ \dfrac{1}{(s+10)^2} & \dfrac{100}{(s+10)^2} \end{bmatrix}. \tag{41}$$

TABLE 5. Minimum value of the objective function J_2 for FO plant with time-delays.

$C(s)$	dc gain of $M(s) \neq I$				dc gain of $M(s) = I$	
	Without SSM		With SSM		Without SSM	
	IO	FO	IO	FO	IO	FO
3 term	2.18	1.56	4.88	0.20	4.22	0.08
4 term	0.83	0.13	4.09	0.18	1.03	0.03
PID	0.17	0.14	n/a	n/a	0.07	0.02
PID[22]	n/a		n/a		0.09	n/a

2) PERFORMANCE EVALUATION OF IOC/FOC FOR FO PLANT WITH TIME-DELAYS

The minimum value of the objective function J_2 defined in (33), obtained for the FO plant presented in (40) has been shown in Table 5. Comparison of the minimum value of the objective function defined in (33), obtained using the method presented in [22] with the corresponding value obtained using the proposed method, is given in Table 5. The IOPID in [22] had different denominator polynomials in each element of its TFM, which thereby increases the overall order of the MIMO system. In this work, $C(s)$ is designed to have the same denominator polynomial in each element of its TFM which results in its minimum realization. The proposed controller design method outperforms the method presented in [22] on realization and ISE index. In addition, the performance of FOC while compared with its IO counterpart is found superior because of its better ISE index.

The IOPID controller designed using the proposed method is, C(s), as shown at the bottom of the next page.

In Table 5, the minimum value of optimum ISE indices has been obtained for the following FOPID, C(s), as shown at the bottom of the next page.

The investigation on the capabilities of the controller to achieve the desired closed-loop characteristics in the presence of load disturbance is of prime importance in controller design procedures. A load disturbance signal $D(s) = [D_1(s)\ D_2(s)]^T$ has been applied to the system as shown

$$C(s) = \frac{1}{s^{2.6} + 0.094842s^{1.9} + 5.2517s + 0.13064} \times \begin{bmatrix} 0.39269s^{1.2} + 0.048878s^{0.6} + 1.55 & 0.029274s^{1.7} + 0.047107s^{0.6} + 0.014087 \\ 0.044781s^{1.4} + 0.053418s^{0.2} - 0.0080568 & 0.53433s^{1.1} - 0.11485s^{0.9} + 1.5589 \end{bmatrix}$$

$$C(s) = \frac{1}{s^{2.7} + 0.57296s^{1.7} + 5.3617s + 0.13333} \times \begin{bmatrix} 0.11034s^{1.7} + 0.43778s^{0.9} + 1.5916 & 0.043811s^{1.8} + 0.069231s^{0.4} + 0.00023976 \\ 0.046149s^{1.8} + 0.074233s^{0.5} + 0.0096455 & 0.46353s^{1.1} + 0.066982s^{0.2} + 1.5577 \end{bmatrix}$$

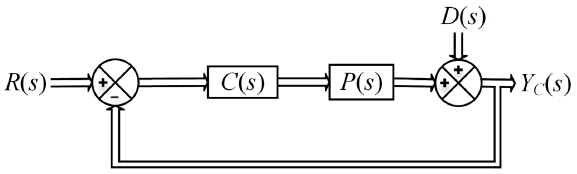

FIGURE 6. Designed closed-loop system with load disturbance.

in Fig. 6, to assess the disturbance rejection characteristics of the proposed controller. The load disturbance signal D_1 occurs on first output y_1 at 4 s and 10 s with magnitude +10% and −10% of the steady-state value of y_1 respectively, each with 2 s duration, as shown in Fig. 7. The load disturbance signal D_2 on second output y_2 is kept as zero. The effect of D_1 on y_1 and y_2 are shown in Figs. 7(a) and 7(b) respectively, which indicate the satisfactory disturbance rejection capabilities of the proposed controller. The disturbance rejection capabilities of the proposed controller design technique are demonstrated for the four-term FOC. The user-defined reference model presented in [22] is used for the controller design in this case.

From the simulation of the closed-loop system with the designed FOC/IOC for IO/FO MIMO plant with time-delays, it is evident that the performance of the designed closed-loop system matches with that of the reference model. The superiority in performance of the FOC over its IO counterpart is evident from the comparison of the closed-loop step responses based on the ISE index.

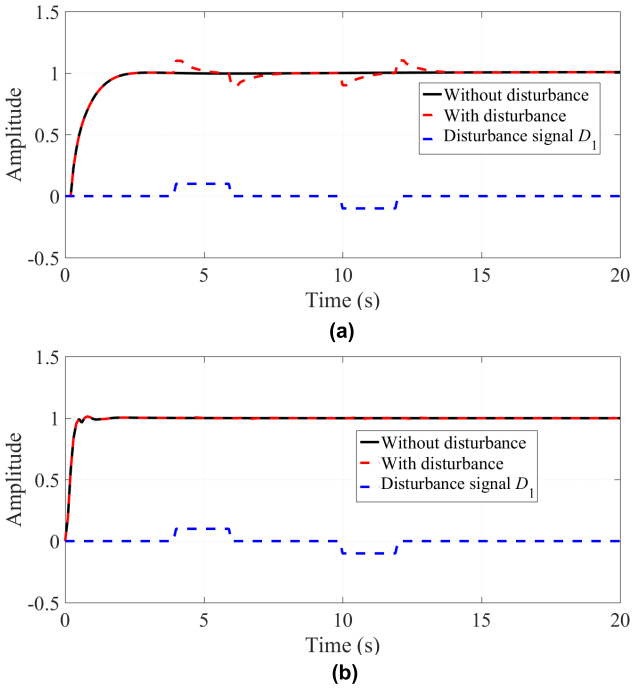

FIGURE 7. Comparison of the output responses of the designed closed-loop system with and without disturbance at (a) output 1 due to D_1 (b) output 2 due to D_1.

VI. EXPERIMENTAL RESULTS: MIMO IO PLANT WITH TIME-DELAYS

The experimental verification of the obtained controller parameters is performed for a wheeled mobile robot QBot 2. The working of QBot 2 is already discussed in [40]. The MATLAB-based Simulink, interfaced with the experimental setup of a wheeled mobile robot is utilized to illustrate the performance of the designed controller. The real-time control software, QUARC, downloads real-time code which is generated from the host computer, into an embedded computer mounted on the QBot 2 platform [40]. The velocity profiles of wheeled mobile robot, while the four-term FOC was designed to match the steady-state response of designed-closed loop system with that of the reference model and the GIM chose was having IO representation have been shown in Figs. 8(a)-8(b). It clearly shows the velocity profiles of the right and left wheels of the wheeled mobile robot during simulation, and experimental analysis matches well with the velocity profiles of the reference model. The deviation present in the experimental result is more, compared with that present in the simulation results, which may be due to the modeling error incorporated during the formulation of the mathematical representation of the plant dynamics. The controller effort present at the right and left wheels of the wheeled mobile robot during the experimental analysis have been shown in Figs. 9(a) and 9(b), respectively. The controller effort measured was for the four-term FOC/IOC, which was designed to match the steady-state response of

$$C(s) = \frac{1}{s^2 + 0.59559s} \times \begin{bmatrix} 0.053723s^2 + 2.0881s + 0.26706 & 9.6131s^2 + 9.8827s + 2.109 \\ 2.3408s^2 + 2.3959s + 0.34254 & -2.8443s^2 - 7.8359s - 1.3578 \end{bmatrix}$$

$$C(s) = \frac{1}{s^{1.2} + 1.1765 \times 10^{-05} s^{0.2}} \times \begin{bmatrix} -3.5798s^{1.2} + 5.3282s - 1.6614s^{0.4} + 1.3964s^{0.2} - 0.044051 \\ 5.0304s^{1.2} - 10.996s + 8.914s^{0.9} + 0.15828s^{0.2} + 0.09343 \\ 33.123s^{1.2} - 53.937s^{1.1} + 31.613s + 2.4282s^{0.2} + 0.35909 \\ 0.0057557s^{1.2} - 3.4458s - 5.0593s^{0.4} + 1.4106s^{0.2} - 0.4139 \end{bmatrix}$$

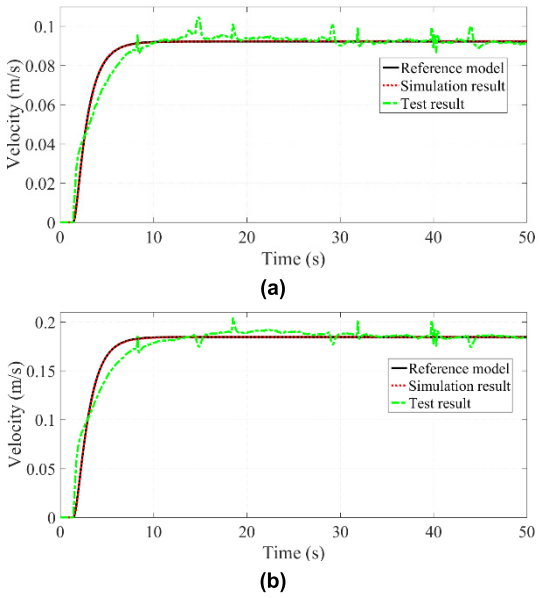

FIGURE 8. Comparison between simulation results and experimental results of the wheeled mobile robot velocity profiles. (a) left wheel. (b) right wheel.

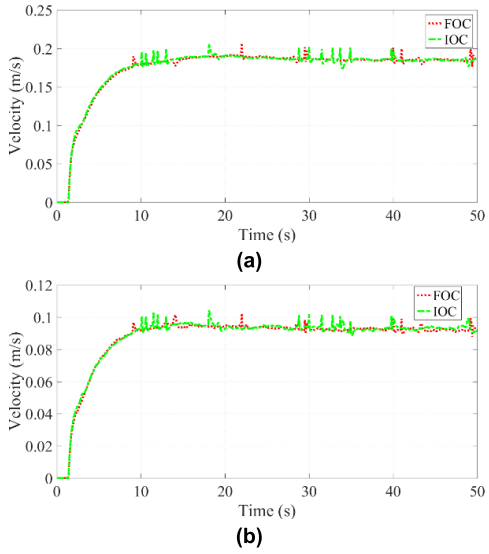

FIGURE 9. Controller effort at (a) right wheel (b) left wheel.

the designed-closed loop system with that of the reference model and while IO representation was chosen for the GIM. The comparison of the performances of the controllers during experimental analysis has been performed based on integral squared control effort. For the right wheel of the wheeled mobile robot, the values obtained for the integral squared control effort are 15.6721 and 15.7419 for FOC and IOC, respectively, while the corresponding values for the left wheel are 3.9384 and 3.9857. The lesser integral squared control effort and hence the lower energy consumption is obtained with FOC in comparison of that with its IO counterpart.

VII. CONCLUSIONS

This paper deals with the design of a model-matching FOC/IOC using AGTM/AGMP matching technique. The proposed FOC/IOC design approach belongs to the class of generalized algebraic method. The proposed reference model selection procedure guarantees a solution for every set of feasible desired specifications of the designed closed-loop system. The reference model selection procedure and controller design approach presented in this work are generalized one and hence applies to IO/FO SISO/MIMO linear plant with or without time-delays. The load disturbance rejection capability and the robustness to system parameter variations offered by the proposed controller are evident from the simulation results. The reference model selection procedure and controller design approach are proved to be efficient and accurate by simulation and experimental results. The future research plan includes the development and implementation of the proposed controller design algorithm for SISO/MIMO IO/FO interval plant with or without time-delays.

APPENDIX

An outline of the optimization framework of the reference model selection procedure using the global optimization toolbox of MATLAB is presented in this section. The optimal set of decision variables can be determined by heuristic search methods, and the genetic algorithm has been used in this work. The bounds for the interaction factor of the GIM and elements of diagonal weighting matrices of the GLCLS model are given as 5×10^{-7} and inf, respectively. The interaction parameters of the GIM are assumed to be identical. The lower and upper bounds for α in the case of FO GIM are given as zero and one, respectively. MATLAB function "lqr" is utilized to obtain the value of gain matrix K_{opt}. The feedback gain matrix can be obtained for a given set of weighting matrices Q and R, by solving the algebraic Riccati equation. The solution of the algebraic Riccati equation is determined using the method presented in [39].

Case 1: IO REPRESENTATION OF GIM

The optimal value of the interaction parameter λ of the GIM is obtained as 1589.5. The weighting matrices Q and R of the GLCLS model, are obtained as diag$(0, 2.4414\times10^{-04}, 6.2671, 6.1746, 10.1043, 9.9536)$ and diag$(20.6833, 20.3829)$, respectively.

Case 2: FO REPRESENTATION OF GIM

The optimal value of the interaction parameter λ of the GIM is obtained as 233.5492. The weighting matrices of the GLCLS model, Q and R are obtained as diag(0.2743, 0.2390, 98.5533, 86.3534, 123.2557, 106.0006) and diag(1.0233, 9.9584), respectively. The parameter $\alpha$of the FO GIM is obtained as 0.87. The obtained optimal parameters together with the desired time-domain specifications are utilized to obtain the GIM and the GLCLS model as described in section III.

REFERENCES

[1] R. Scherer, S. L. Kalla, Y. Tang, and J. Huang, "The Grünwald–Letnikov method for fractional differential equations," *Comput. Math. Appl.*, vol. 62, no. 3, pp. 902–917, Aug. 2011.

[2] H. K. Abdulkhader, J. Jacob, and A. T. Mathew, "Fractional-order lead-lag compensator-based multi-band power system stabiliser design using a hybrid dynamic GA-PSO algorithm," *IET Gener., Transmiss. Distrib.*, vol. 12, no. 13, pp. 3248–3260, Jul. 2018.

[3] C. A. Monje, Y. Chen, B. M. Vinagre, D. Xue, and V. Feliu-Batlle, *Fractional-order Systems and Controls: Fundamentals and Applications*. London, U.K.: Springer, 2010.

[4] R. M. Stefanescu, C. L. Prioroc, and A. M. Stoica, "Weighting matrices determination using pole placement for tracking maneuvers," *Univ. Politehnica Bucharest Sci. Bull., D*, vol. 75, no. 2, pp. 31–41, 2013.

[5] H. R. Pourshaghaghi, M. R. Jaheh-Motlagh, and A. Jalali, "Optimal feedback control design using genetic algorithm applied to inverted pendulum," in *Proc. IEEE Int. Symp. Ind. Electron.*, Vigo, Spain, Jun. 2007, pp. 263–268.

[6] K. Hassani and W. S. Lee, "Optimal tuning of linear quadratic regulators using quantum particle swarm optimization," in *Proc. Int. Conf. Control, Dyn. Syst., Robot. (CDSR)*, May 2014, pp. 1–8.

[7] S. B. Quinn, Jr., and C. K. Sanathanan, "Model matching control for multivariable systems—I. Stable plants," *J. Franklin Inst.*, vol. 327, no. 5, pp. 699–712, Jan. 1990.

[8] S. Damodaran, T. K. S. Kumar, and A. P. Sudheer, "Design and implementation of GA tuned PID controller for desired interaction and trajectory tracking of wheeled mobile robot," in *Proc. Adv. Robot. (AIR)*, Jun. 2017, Art. no. 34.

[9] S. M. Joshi, G. Tao, and P. Patre, "Direct adaptive control using an adaptive reference model," *Int. J. Control*, vol. 84, no. 1, pp. 180–196, Jan. 2011.

[10] A. B. Maamri and J. C. Trigeassou, "Design of PID controllers for delayed MIMO plants using moments based approach," *J. Elect. Eng.*, vol. 57, no. 6, pp. 318–328, 2006.

[11] A. Oustaloup, *La Commande CRONE: CommandeRobusted'ordre NonEntier, Paris*. Paris, France: Hermès, 1991.

[12] I. Podlubny, "Fractional-order systems and $PI^{\lambda}D^{\mu}$ -controllers," *IEEE Trans. Autom. Control*, vol. 44, no. 1, pp. 208–214, Jan. 1999.

[13] H. Liu, Y. Pan, S. Li, and Y. Chen, "Adaptive fuzzy backstepping control of fractional-order nonlinear systems," *IEEE Trans. Syst., Man, Cybern., Syst.*, vol. 47, no. 8, pp. 2209–2217, Aug. 2017.

[14] H. Liu, Y. Pan, S. Li, and Y. Chen, "Synchronization for fractional-order neural networks with full/under-actuation using fractional-order sliding mode control," *Int. J. Mach. Learn. Cybern.*, vol. 9, no. 7, pp. 1219–1232, Jul. 2018.

[15] S. Das, *Functional Fractional Calculus*. Berlin, Germany: Springer, 2011.

[16] M. Beschi, F. Padula, and A. Visioli, "The generalised isodamping approach for robust fractional PID controllers design," *Int. J. Control*, vol. 90, no. 6, pp. 1157–1164, Jun. 2017.

[17] Z. Yakoub, M. Chetoui, M. Amairi, and M. Aoun, "Model-based fractional order controller design," *IFAC-PapersOnLine*, vol. 50, no. 1, pp. 10431–10436, Jul. 2017.

[18] S. B. Quinn, Jr., and C. K. Sanathanan, "Model matching control for multivariable systems—II. Unstable plants," *J. Franklin Inst.*, vol. 327, no. 5, pp. 713–729, 1990.

[19] G. Szita and C. K. Sanathanan, "A model matching approach for designing decentralized MIMO controllers," *J. Franklin Inst.*, vol. 337, no. 6, pp. 641–660, Sep. 2000.

[20] G. Szita and C. K. Sanathanan, "Model matching controller design for disturbance rejection," *J. Franklin Inst.*, vol. 333, no. 5, pp. 747–772, Sep. 1996.

[21] S. K. Das, H. R. Pota, and I. R. Petersen, "Multivariable negative-imaginary controller design for damping and cross coupling reduction of nanopositioners: A reference model matching approach," *IEEE/ASME Trans. Mechatronics*, vol. 20, no. 6, pp. 3123–3134, Dec. 2015.

[22] D. Xue and T. Li, "An approach to design controllers for MIMO fractional-order plants based on parameter optimization algorithm," *ISA Trans.*, vol. 82, pp. 145–152, Nov. 2018.

[23] L. Liu, S. Zhang, D. Xue, and Y. Q. Chen, "General robustness analysis and robust fractional-order PD controller design for fractional-order plants," *IET Control Theory Appl.*, vol. 12, no. 12, pp. 1730–1736, Aug. 2018.

[24] K. Dheeraj, J. Jacob, and M. P. Nandakumar, "Direct adaptive neural control design for a class of nonlinear multi input multi output systems," *IEEE Access*, vol. 7, pp. 15424–15435, Jan. 2019. doi: 10.1109/ACCESS.2019.2892460.

[25] H.-P. Ren, J.-T. Fan, and O. Kaynak, "Optimal design of a fractional order PID controller for a pneumatic position servo system," *IEEE Trans. Ind. Electron.*, to be published. doi: 10.1109/TIE.2018.2870412.

[26] M. Dulău, A. Gligor, and T. M. Dulău, "Fractional order controllers versus integer order controllers," *Procedia Eng.*, vol. 181, pp. 538–545, Jan. 2017.

[27] A. S. Chopade, S. W. Khubalkar, A. S. Junghare, M. V. Aware, and S. Das, "Design and implementation of digital fractional order PID controller using optimal pole-zero approximation method for magnetic levitation system," *IEEE/CAA J. Autom. Sinica*, vol. 5, no. 5, pp. 977–989, Sep. 2018.

[28] A. Rojas-Moreno, "An approach to design MIMO FO controllers for unstable nonlinear plants," *IEEE/CAA J. Autom. Sinica*, vol. 3, no. 3, pp. 338–344, Jul. 2016.

[29] J. Pal, "An algorithmic method for the simplification of linear dynamic scalar systems," *Int. J. Control*, vol. 43, no. 1, pp. 257–269, Jan. 1986.

[30] J. Pal, B. Sarvesh, and M. K. Ghosh, "A new method for model order reduction," *IETE J. Res.*, vol. 41, nos. 5–6, pp. 305–311, Sep./Dec. 1995.

[31] M. Khanra, J. Pal, and K. Biswas, "Reduced order approximation of MIMO fractional order systems," *IEEE J. Emerg. Sel. Top. Circuits Syst.*, vol. 3, no. 3, pp. 451–458, Sep. 2013.

[32] C. K. Sanathanan and S. B. Quinn, Jr., "Controller design via the synthesis equation," *J. Franklin Inst.*, vol. 324, no. 3, pp. 431–451, Jan. 1987.

[33] D. Chen and D. E. Seborg, "PI/PID controller design based on direct synthesis and disturbance rejection," *Ind. Eng. Chem. Res.*, vol. 41, no. 19, pp. 4807–4822, Sep. 2002.

[34] M. N. Anwar, M. Shamsuzzoha, and S. Pan, "A frequency domain PID controller design method using direct synthesis approach," *Arabian J. Sci. Eng.*, vol. 40, no. 4, pp. 995–1004, Apr. 2015.

[35] A. Jajarmi and D. Baleanu, "Suboptimal control of fractional-order dynamic systems with delay argument," *J. Vib. Control*, vol. 24, no. 12, pp. 2430–2446, Jun. 2018.

[36] J. L. Peczkowski, "Multivariable synthesis with transfer functions," in *Proc. Propuls. Controls Symp.*, May 1979, pp. 111–128.

[37] F. Merrikh-Bayat and M. Karimi-Ghartemani, "Some properties of three-term fractional order system," *Fractional Calculus Appl. Anal.*, vol. 11, no. 3, pp. 317–328, Sep. 2008.

[38] F. J. Rytkonen, "Modern control regulator design for DC-DC converters," Ph.D. dissertation, Dept. Electr. Comput. Eng., Portland State Univ., Portland, OR, USA, 2005.

[39] M. C. Priess, R. Conway, J. Choi, J. M. Popovich, and C. Radcliffe, "Solutions to the inverse LQR problem with application to biological systems analysis," *IEEE Trans. Control Syst. Technol.*, vol. 23, no. 2, pp. 770–777, Mar. 2015.

[40] *QBot 2 for QUARC Set Up and Configuration*, Quanser, Markham, ON, Canada, 2015.

SURAJ DAMODARAN was born in 1983. He received the B.Tech. degree in applied electronics and instrumentation engineering from Kerala University, Thiruvananthapuram, India, in 2005, and the M.Tech. degree in electrical engineering from the National Institute of Technology, Calicut, in 2009. He has served as an Adhoc Lecturer with the National Institute of Technology (2009–2010), and also with the Vidya Academy of Science and Technology (2010–2013), where he has been a Research Scholar with the Department of Electrical Engineering, since 2013. His main research interests include the application of Control Theory to the robotic systems, model-order reduction, genetic algorithms, model-matching control, and fractional-order control. He is a member of The Robotics Society, India.

THAZHE KUNNATH SUNIL KUMAR was born in Calicut, India, in 1974. He received the B.Tech. degree in electrical engineering from Calicut University, Thenjipalam, India, in 1997, the M.Tech. degree in power systems from Ranchi University, Jamshedpur, in 2001, and the Ph.D. degree in electrical engineering from IIT Kharagpur, India, in 2009. He is currently an Assistant Professor with the Department of Electrical Engineering, National Institute of Technology, Calicut, India. His main research interests include the application of control theory and computers to the power systems, model-order reduction, genetic algorithms, PID tuning, random search optimization, controller design in 2-DOF configuration, fractional-order control, and interval systems. He is a Life Member of the Systems Society of India.

ATTADAPPA PUTHANVEETIL SUDHEER received the B.Sc. degree in mathematics from Calicut University, in 1992, the B.Tech. degree in mechanical engineering from Mahatma Gandhi University, in 1996, the M.E. degree in manufacturing engineering from Anna University, in 2005, and the Ph.D. degree in humanoid robotics from the Department of Mechanical Engineering, National Institute of Technology, Calicut, India, in 2015, where he is currently an Assistant Professor. He has reputed publications and patents in the area of robotics/mechatronics systems. His major research interests include kinematics, dynamics, and control of robotic systems, vision systems, and intelligent locomotion of mobile robots. He is currently the Editor of The Robotics Society, India.